



ELSEVIER

Journal of Magnetism and Magnetic Materials 248 (2002) 19–25



www.elsevier.com/locate/jmmm

Cerium influence on the spin reorientation in $\text{Er}_{2-x}\text{Ce}_x\text{Fe}_{14}\text{B}$ evidenced by Mössbauer and DSC techniques

A.T. Pędziwiatr*, B.F. Bogacz, R. Gargula, S. Wróbel

Institute of Physics, Jagiellonian University, Reymonta 4, 30-059 Cracow, Poland

Received 4 October 2001; received in revised form 27 November 2001

Abstract

Polycrystalline $\text{Er}_{2-x}\text{Ce}_x\text{Fe}_{14}\text{B}$ ($x = 0.25, 0.5, 1.0$) compounds have been studied by ^{57}Fe Mössbauer spectroscopy and by differential scanning calorimetry (DSC) in the temperature range 80–470 K. The spin reorientation phenomenon has been studied extensively by narrow step temperature scanning in the vicinity of the spin reorientation temperature. It was found that in the region of transition, each Mössbauer subspectrum splits into two Zeeman sextets, which are characterised by different hyperfine magnetic fields and quadrupole splittings. A consistent way of describing the Mössbauer spectra in the reorientation region, below and above, was proposed. The composition and temperature dependencies of hyperfine interaction parameters and subspectra contributions were derived from experimental spectra.

The endothermic DSC peaks were observed for all studied compounds, which correspond to the transition from basal plane to axial easy magnetisation direction on increasing the temperature. The spin reorientation temperatures and the enthalpies of transitions were established from DSC data. The spin arrangement diagram was constructed and the spin reorientation temperatures obtained by the two methods were compared. © 2002 Elsevier Science B.V. All rights reserved.

PACS: 75.50.Ww; 76.80.+y; 64.60.-i

Keywords: Permanent magnet materials; Mössbauer effect; Spin reorientation; DSC

1. Introduction

The studies of spin reorientation phenomena in $\text{R}_2\text{Fe}_{14}\text{B}$ -type (R = rare earth) compounds are important from a fundamental point of view and also for permanent magnet applications. These magnetic transitions originate because of different temperature dependencies of the iron and rare

earth sublattice anisotropies. Until now, several groups [1–10] have studied the nature of spin reorientation phenomena in $\text{Er}_2\text{Fe}_{14}\text{B}$. In this compound, the magnetocrystalline anisotropy changes from planar to axial along the c -axis when the temperature increases at about 316 K [1].

The easy magnetisation direction of $\text{Er}_2\text{Fe}_{14}\text{B}$ depends on a temperature-induced competition between the uniaxial Fe sublattice anisotropy [11] and the basal plane Er sublattice anisotropy [12].

In this paper, we present a study of $\text{Er}_{2-x}\text{Ce}_x\text{Fe}_{14}\text{B}$ compounds. These compounds have

*Corresponding author. Tel.: +48-12-632-4888x5505; fax: +48-12-633-7086.

E-mail address: ufpedziw@if.uj.edu.pl (A.T. Pędziwiatr).

$\text{Nd}_2\text{Fe}_{14}\text{B}$ -type crystal structure, which is tetragonal, belonging to space group $\text{P4}_2/\text{mnm}$. The rare earth ions occupy two distinct crystallographic sites (4f and 4g), the iron atoms share six non-equivalent positions (16k₁, 16k₂, 8j₁, 8j₂, 4e, 4c) and boron is located at one type of site (4g) [13]. Recent study by single crystal neutron diffraction on $\text{Er}_2\text{Fe}_{14}\text{B}$ [14] revealed that there is a change of crystal structure to orthorhombic below the spin reorientation transition.

Previous investigations showed that $\text{Ce}_2\text{Fe}_{14}\text{B}$ possesses an anomalously small lattice volume contrary to predictions based on the lanthanide contraction for the series of R^{3+} -based compounds. Mössbauer measurements of $\text{Er}_{2-x}\text{Ce}_x\text{Fe}_{14}\text{B}$ at 295 and 78 K [15] show that spin transition causes changes in the shape of experimental spectra. In particular, the sixth line of 8j₂ sextet is well resolved in the case of the axial spin arrangement.

We conducted a systematic study of the $\text{Er}_{2-x}\text{Ce}_x\text{Fe}_{14}\text{B}$ ($x = 0.25, 0.5, 1.0$) compounds in the vicinity of the spin reorientation temperature using Mössbauer effect and differential scanning calorimetry (DSC), trying to establish the influence of cerium on the transition and to reveal thermal effects connected with this transition.

2. Experimental details

The $\text{Er}_{2-x}\text{Ce}_x\text{Fe}_{14}\text{B}$ alloys ($x = 0.25, 0.5, 1.0$) were produced by a standard procedure of induction melting under flowing high-purity argon and subsequent annealing at 900°C for 2 weeks. The X-ray and thermomagnetic analyses proved the single phase integrity of materials. The ^{57}Fe Mössbauer transmission spectra were recorded in the temperature range 80–330 K. The spin reorientation phenomenon near T_{SR} has been studied extensively by narrow step (5, 10 K) temperature scanning using a $^{57}\text{Co}(\text{Rh})$ source and a computer-driven constant acceleration mode spectrometer. A high-purity iron foil was used to calibrate the velocity scale. Isomer shifts were established with respect to the centre of gravity of the room temperature iron Mössbauer spectrum. Samples of $\text{Er}_{2-x}\text{Ce}_x\text{Fe}_{14}\text{B}$ ($x = 0.25, 0.5, 1.0$) have also

been studied by DSC in the temperature range 170–470 K. The measurements were performed in heating and cooling cycles at rates ranging from 5 to 60 K/min.

3. Data analysis

The selected experimental Mössbauer spectra of the $\text{Er}_{1.75}\text{Ce}_{0.25}\text{Fe}_{14}\text{B}$ and $\text{ErCeFe}_{14}\text{B}$ intermetallic compounds are shown in Figs. 1 and 2, respectively. The “exponential” approximation [16] of the transmission integral was used to describe the investigated Mössbauer spectra, similarly as in

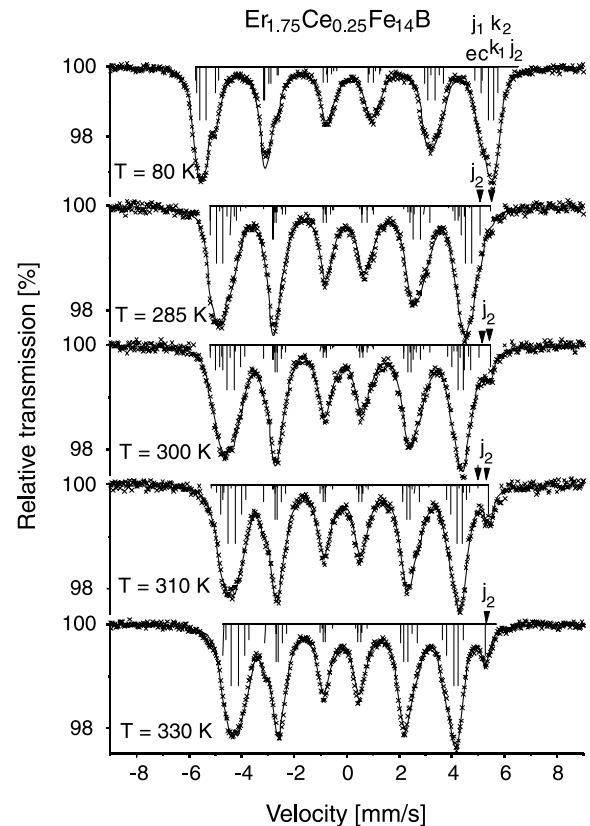


Fig. 1. The selected ^{57}Fe Mössbauer transmission spectra for the $\text{Er}_{1.75}\text{Ce}_{0.25}\text{Fe}_{14}\text{B}$ intermetallic compound. The solid lines are fits to the data. The stick diagrams show the line positions and relative intensities. Positions of the sixth line of 8j₂ sextets are specially marked. In the transition region, 8j₂ has two positions, corresponding to “low” and “high temperature” Zeeman sextets, marked by arrows.

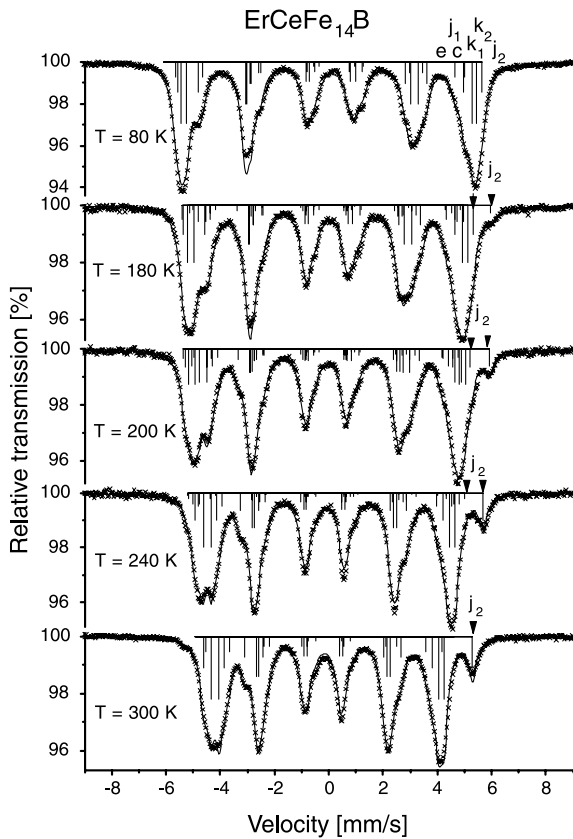


Fig. 2. The selected ^{57}Fe Mössbauer transmission spectra for the $\text{ErCeFe}_{14}\text{B}$ intermetallic compound. The solid lines are fits to the data. The stick diagrams show the line positions and relative intensities. Positions of the sixth line of $8j_2$ sextets are specially marked. In the transition region, $8j_2$ has two positions, corresponding to “low” and “high temperature” Zeeman sextets, marked by arrows.

Refs. [10,17]. A simultaneous fitting of several Mössbauer spectra gave opportunity to establish a consistent description of all spectra and the temperature dependence of hyperfine interaction parameters. The spectra below and above the region of spin reorientation were analysed using six Zeeman subspectra with relative intensities in agreement with iron occupation of crystallographic sublattices (4:4:2:2:1:1). Each subspectrum was characterised by the following hyperfine interaction parameters: magnetic field, B , isomer shift, δ , quadrupole splitting, 2ε (defined as $[(V_6 - V_5) - (V_2 - V_1)]/2$, where V_i are the velocities

corresponding to the position of the Mössbauer lines).

It is observed that the amplitude of the sixth, separated line of the $8j_2$ Zeeman sextet (Figs. 1 and 2) changes its value as the temperature increases in the transition region, which is the result of the splitting of $8j_2$ Zeeman sextet into two parts, similar to what was described for $\text{Er}_{2-x}\text{Y}_x\text{Fe}_{14}\text{B}$ compounds [10,17]. Thus, we used the following procedure, which allowed us to observe direct changes in the shape of Mössbauer spectra: two spectra of the same compound recorded at different temperatures were numerically subtracted. The procedure of subtraction was preceded by the correction of the subtracted spectrum which took into consideration the temperature changes of δ and B . Values of changes per 1 K ($\Delta\delta/\Delta T$, $\Delta B/\Delta T$) were determined on the basis of the analysis of Mössbauer spectra recorded beyond the spin reorientation region. Selected results of the subtraction of spectra taken at different temperatures for the $\text{ErCeFe}_{14}\text{B}$ are shown in Fig. 3. The temperature correction of δ and B in the spectrum taken at higher temperature was introduced. In the first graph (140–150 K) these spectra subtract almost entirely. “Differential spectra” obtained at higher temperatures (180–190, 190–200, 200–210 and 210–220 K) show visible changes occurring during reorientation. In the presented “differential spectra”, the lines that disappear during the reorientation process (with increasing temperature) are observed in the form of “absorption” lines and the lines that appear after the spin reorientation are observed in the form of “scattering” lines. The last graph in Fig. 3 (270–280 K) represents the end of the spin reorientation process: changes are no longer visible. The analysis presented above shows that the reorientation process occurs in a range of temperature. It was observed that changes in the right part of the spectrum concern mainly the position of the sixth line of the $8j_2$ sextet. It is difficult to attribute other changes to a concrete, one distinct sublattice. Thus, we conclude that all sublattices take part in the spin reorientation collectively. This direct observation of changes in the experimental Mössbauer spectra during spin reorientation allows to propose the following idea

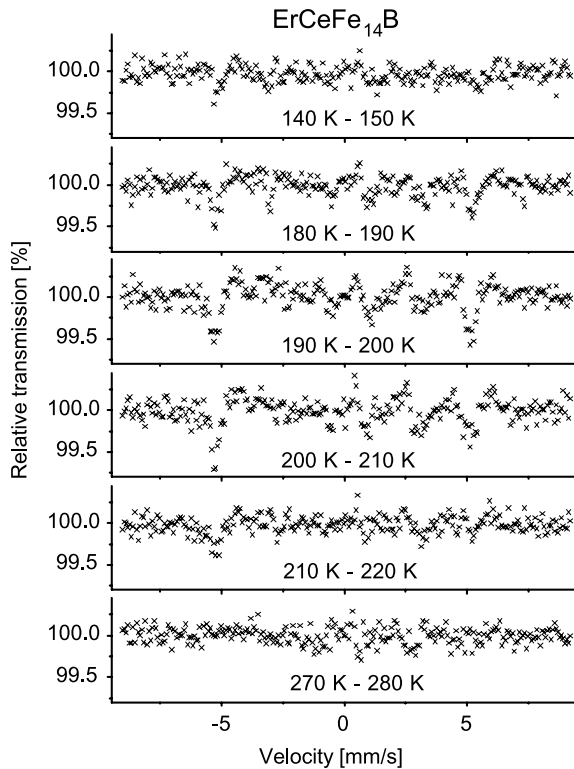


Fig. 3. The selected differential spectra for $\text{ErCeFe}_{14}\text{B}$. The lines disappearing during reorientation process (with the increase of temperature) are observed in the form of “absorption” lines and the lines appearing after spin reorientation are observed in the form of “scattering” lines.

of description: spectra recorded at temperatures below the transition (planar spin arrangement) are described by “low temperature” sextets and spectra recorded at temperatures above the transition (axial spin arrangement) are described by “high temperature” Zeeman sextets. There is a coexistence of the “low” and “high temperature” Zeeman sextets in the transition region. Both kinds of Zeeman sextets exchange gradually (between themselves) their contributions C_l , C_h to the total spectrum and have different values of B and 2ε . The weak, systematic changes of B and 2ε with temperature are taken into account to fit the spectra below and above the spin reorientation region. A common linear temperature dependence of δ caused by second-order Doppler shift effect is

assumed for “low” and “high temperature” Zeeman sextets. No noticeable changes of linewidths are observed in the fitting procedure. A slight misfit at ~ -2.5 mm/s may be caused by the constraint and simplification of the temperature dependence of Mössbauer parameters in the applied model of description. This description is similar to the procedure applied for polycrystalline $\text{Er}_{2-x}\text{Y}_x\text{Fe}_{14}\text{B}$ [10,17].

Our goal was also to find the temperature range of the spin reorientation phenomenon and to determine the spin reorientation temperature using Mössbauer analysis. The most useful feature which enables to do this is the separation of the sixth line in the $8j_2$ subspectrum of the analysed experimental spectra. Owing to the clear development of its intensity in the course of the transition, it was possible to establish precisely the contribution of “high temperature” Zeeman part of the $8j_2$ sublattice to the spectrum and to conclude on the spin reorientation temperature.

4. Results and discussion

The contributions C_l , C_h of both “low” and “high temperature” Zeeman sextets, correspondingly, are shown in Fig. 4. From this plot, we derived the spin reorientation temperature (assumed to be at the intersection point of C_l and C_h curves) for $\text{Er}_{2-x}\text{Ce}_x\text{Fe}_{14}\text{B}$ ($x = 0.0$ [10], 0.25, 0.5, 1.0). It was observed that the substitution of Ce for Er causes the decrease of T_{SR} and the increase of the temperature range of spin reorientation (Fig. 4). The values of the spin reorientation temperature determined from Mössbauer measurements, T_{SRM} , for all studied compositions are given in Table 1.

The temperature dependencies of hyperfine magnetic fields derived from the spectra for the $\text{Er}_{2-x}\text{Ce}_x\text{Fe}_{14}\text{B}$ system are shown in Fig. 5. The attribution of B to the crystal sublattices was based on the nearest neighbour argumentation [18]. The hyperfine magnetic field decreases as the temperature increases below and above the spin reorientation region for all sublattices. In the region of transition, we observed experimentally that each Zeeman sextet splits into two parts.

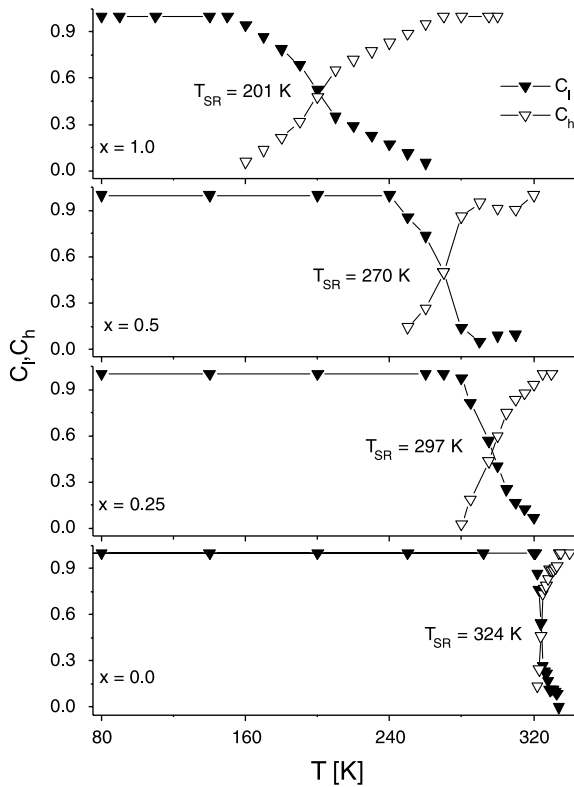


Fig. 4. Temperature dependencies of subspectra contributions for both C_1 —“low temperature” (solid triangle) and C_h —“high temperature” (open triangle) Zeeman sextets. The average error is 0.1.

Table 1

Determined values of spin reorientation temperature: T_{SRM} —by Mössbauer effect, T_{SRK} —by DSC and values of enthalpy of the transition, ΔH , for $Er_{2-x}Ce_xFe_{14}B$ ($x = 0.0$ [10], 0.25, 0.5, 1.0)

Compound	T_{SRM} (K)	T_{SRK} (K)	ΔH (J/g)
$Er_2Fe_{14}B$	324 ± 1	326 ± 1	0.32 ± 0.05
$Er_{1.75}Ce_{0.25}Fe_{14}B$	297 ± 2	302 ± 2	0.10 ± 0.06
$Er_{1.5}Ce_{0.5}Fe_{14}B$	270 ± 3	273 ± 3	0.07 ± 0.06
$ErCeFe_{14}B$	201 ± 5	201 ± 6	—

From a good description of the spectra obtained assuming the presented model, one can conclude on the coexistence of two orientations of the magnetic moments in the reorientation region. Their contributions change with temperature. The introduction of cerium into the samples is the

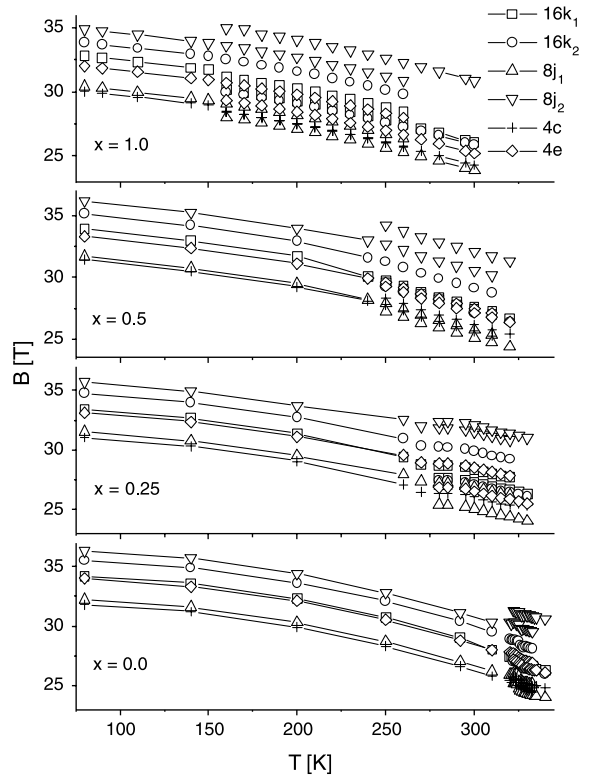


Fig. 5. Temperature dependence of the hyperfine magnetic field B for different crystal sites of the $Er_{2-x}Ce_xFe_{14}B$ ($x = 0.0$ [10], 0.25, 0.5, 1.0). The average error is 0.1 T. The dual assignment in the spin reorientation region is connected with the coexistence of “low” and “high temperature” sextets.

source of statistical, local changes, which can explain the increase of the temperature range of reorientation in samples containing more and more cerium.

The behaviour of 2ε is connected with the change of angle between the easy axis of magnetisation and the electric field gradient [19]. 2ε parameters are almost independent of temperature below and above the region of transition (Fig. 6). For the $8j_2$ sublattice, some changes of 2ε in the initial part of the reorientation region are observed for all $Er_{2-x}Ce_xFe_{14}B$ studied compounds. In the reorientation region, all quadrupole splittings become bigger except for the $16k_1$ sublattice. The change of quadrupole splitting in the reorientation process is the largest for $8j_2$ sublattice. The behaviour of B and 2ε in $Er_{2-x}Ce_xFe_{14}B$

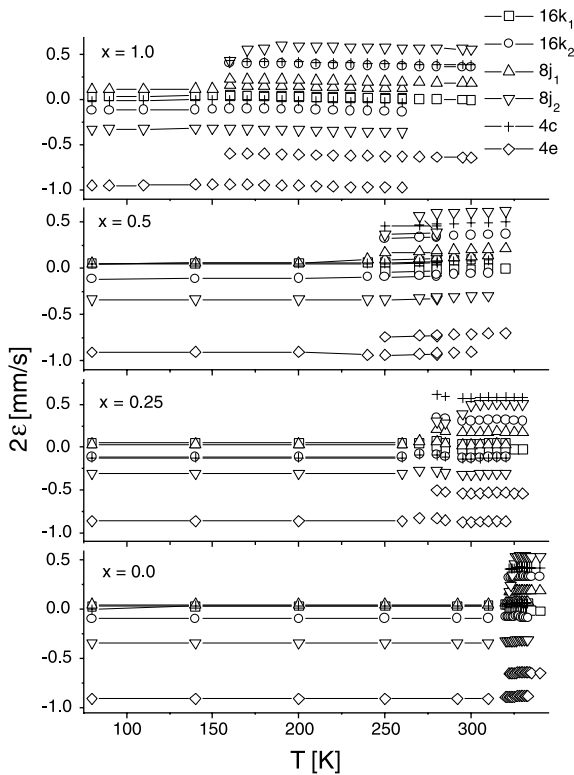


Fig. 6. Temperature dependence of the quadrupole splitting 2ε for different crystal sites of the $\text{Er}_{2-x}\text{Ce}_x\text{Fe}_{14}\text{B}$ ($x = 0.0$ [10], 0.25, 0.5, 1.0). The average error is 0.01 mm/s. The dual assignment in the spin reorientation region is connected with co-existence of “low” and “high temperature” sextets.

($x = 0.25, 0.5, 1.0$) is similar to that observed in $\text{Er}_{2-x}\text{Y}_x\text{Fe}_{14}\text{B}$ [10,17].

Fig. 7 illustrates the selected DSC analysis of thermal effects in $\text{Er}_{1.75}\text{Ce}_{0.25}\text{Fe}_{14}\text{B}$ and $\text{Er}_{1.5}\text{Ce}_{0.5}\text{Fe}_{14}\text{B}$ compounds in the vicinity of spin reorientation. Endothermic peaks correspond to the transition of the easy magnetisation direction from basal plane to c -axis for all studied compounds. The spin reorientation temperature is considered as an arithmetical average temperature of heating (index h) and cooling (index c) peak positions ($T_{\text{SR}} = (T_{\text{SRh}} + T_{\text{SRc}})/2$). The values of the spin reorientation temperature determined from DSC measurements, T_{SRc} , for all studied compounds are given in Table 1. The enthalpy ΔH of the transition (corresponding to the area under the DSC peaks) was calculated

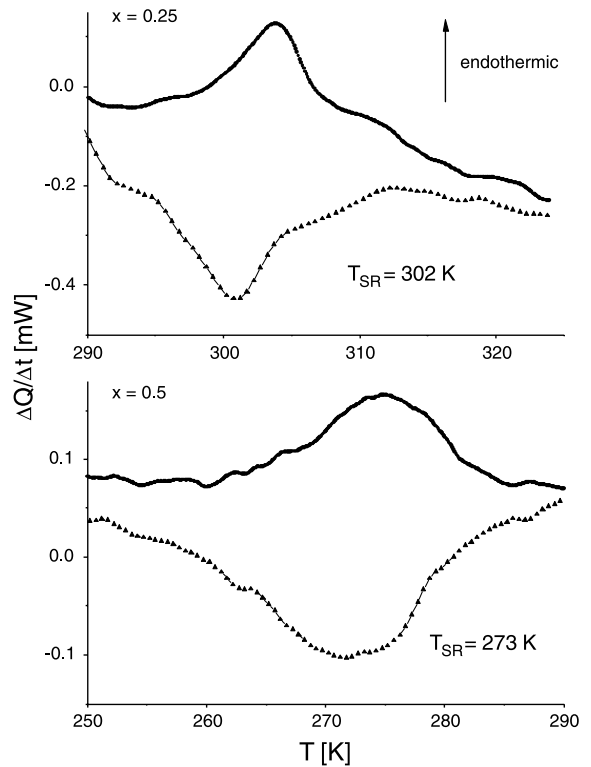


Fig. 7. DSC curves for the $\text{Er}_{2-x}\text{Ce}_x\text{Fe}_{14}\text{B}$ ($x = 0.25, 0.5$) compounds in the spin reorientation region. Upper and lower curves show results of measurements performed on heating (h-indexes) and cooling (c-indexes), respectively, both at a rate of 30 K/min.

as an arithmetical average of the absolute values obtained on heating and cooling. Values of ΔH for $\text{Er}_{2-x}\text{Ce}_x\text{Fe}_{14}\text{B}$ are given in Table 1. Thermal effects connected with spin reorientation were much smaller in $\text{Er}_{2-x}\text{Ce}_x\text{Fe}_{14}\text{B}$ compounds than in $\text{Er}_2\text{Fe}_{14}\text{B}$, which made the estimation of ΔH very difficult. The value of ΔH is comparable with the value of the error in the case of the $\text{Er}_{1.75}\text{Ce}_{0.25}\text{Fe}_{14}\text{B}$ and the $\text{Er}_{1.5}\text{Ce}_{0.5}\text{Fe}_{14}\text{B}$ compounds. The reliable estimation of ΔH was impossible for the $\text{ErCeFe}_{14}\text{B}$ due to a very weak DSC signal.

The spin phase diagram for $\text{Er}_{2-x}\text{Ce}_x\text{Fe}_{14}\text{B}$ systems is shown in Fig. 8. It compares the spin reorientation temperatures obtained by the two methods (Mössbauer effect and DSC), showing a good agreement.

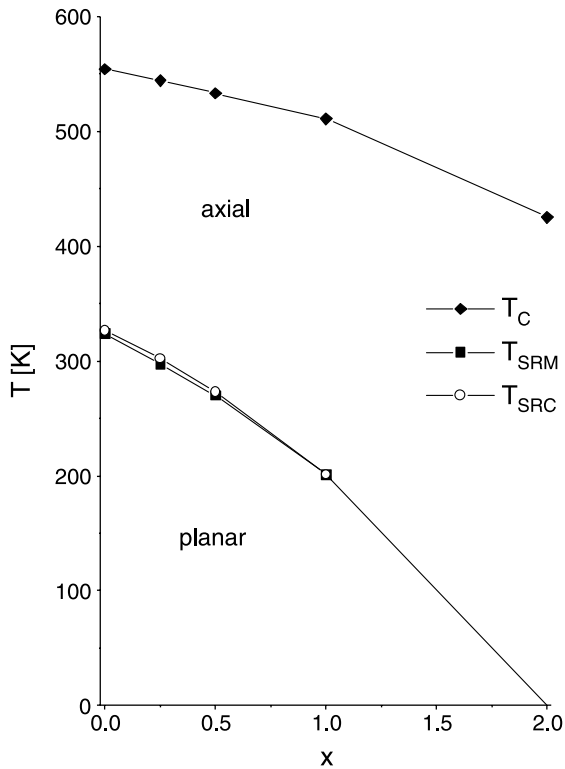


Fig. 8. Spin structure phase diagram for $\text{Er}_{2-x}\text{Ce}_x\text{Fe}_{14}\text{B}$ system: T_C —Curie temperature, T_{SRM} —spin reorientation temperature determined from Mössbauer measurements and T_{SRC} —spin reorientation temperature determined from DSC data.

5. Conclusions

The analysed results suggest that during the reorientation process, the two types of magnetic spin arrangements (axial and planar) coexist and exchange their contributions gradually with temperature. Cerium introduction lowers the spin reorientation temperature and causes an increase

in the temperature range of transition. It also brings damping and broadening of thermal effects, which accompany the transition. Such behaviour of cerium may be attributed to its anomalous size of atomic radius and its electronic structure.

References

- [1] S. Hirosawa, M. Sagawa, *Solid State Commun.* 54 (1985) 335.
- [2] A. Vasquez, J.M. Friedt, J.P. Sanchez, Ph. L'Héritier, R. Fruchart, *Solid State Commun.* 55 (1985) 783.
- [3] E. Burzo, *Rep. Prog. Phys.* 61 (1998) 1099.
- [4] K.H.J. Buschow, *Rep. Prog. Phys.* 54 (1991) 1123.
- [5] C.D. Fuerst, J.F. Herbst, E.A. Alson, *J. Magn. Magn. Mater.* 54–57 (1986) 567.
- [6] J.M. Friedt, A. Vasquez, J.P. Sanchez, P. L'Héritier, R. Fruchart, *J. Phys. F* 16 (1986) 651.
- [7] C. Piqué, R. Burriel, L.M. García, F.J. Lázaro, J. Bartolomé, *J. Magn. Magn. Mater.* 104 (1992) 1167.
- [8] X.C. Kou, E.H.C.P. Sinnecker, R. Grössinger, *J. Magn. Magn. Mater.* 147 (1995) L231.
- [9] Y.B. Kim, Jin Han-min, *J. Magn. Magn. Mater.* 222 (2000) 39.
- [10] R. Wielgosz, A.T. Pędziwiatr, B.F. Bogacz, S. Wróbel, *Mol. Phys. Rep.* 30 (2000) 167.
- [11] D. Givord, H.S. Li, R. Perrier de la Bâthie, *Solid State Commun.* 51 (1984) 857.
- [12] S. Hirosawa, Y. Matsuura, H. Yamamoto, S. Fujimura, M. Sagawa, H. Yamauchi, *J. Appl. Phys.* 59 (1986) 873.
- [13] J.F. Herbst, J.J. Croat, F.E. Pinkerton, W.B. Yelon, *Phys. Rev. B* 29 (1984) 4176.
- [14] P. Wolfers, M. Bacmann, D. Fruchart, *J. Alloys Compounds* 317–318 (2001) 39.
- [15] J.J. Bara, B.F. Bogacz, A.T. Pędziwiatr, *J. Alloys Compounds* 232 (1996) 101.
- [16] B.F. Bogacz, *Mol. Phys. Rep.* 30 (2000) 15.
- [17] A.T. Pędziwiatr, B.F. Bogacz, R. Gargula, S. Wróbel, *J. Alloys Compounds*, in preparation.
- [18] G.J. Long, F. Grandjean, *Supermagnets—Hard Magnetic Materials*, NATO ASI Series, Kluwer Academic Publishers, Dordrecht, 1990, p. 261.
- [19] P. Gülich, R. Link, A. Trautwein, *Mössbauer Spectroscopy and Transition Metal Chemistry*, Springer, Berlin, Heidelberg, New York, 1978.